Biophysical Journal, Volume *118*

Supplemental Information

A Disorder-to-Order Transition Mediates RNA Binding of the *Caenorhabditis elegans* Protein MEX-5

Davide Tavella, Asli Ertekin, Hila Schaal, Sean P. Ryder, and Francesca Massi

A disorder-to-order transition mediates RNA-binding of the *Caenorhabditis elegans* protein MEX-5

Davide Tavella, Asli Ertekin, Hila Schaal, Sean P. Ryder and Francesca Massi

SUPPORTING INFORMATION

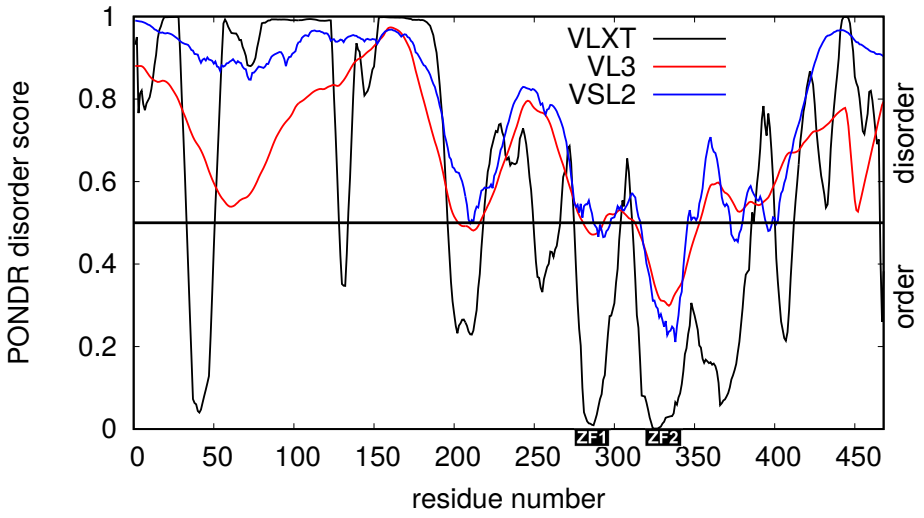

Figure S1: Disorder prediction of MEX-5 estimated using PONDR®. For the three predictors VLXT, VSL2 and VL3, which evaluate the per residue disorder probability, scores above 0.5 correspond to the predicted disordered regions/residues, whereas scores below 0.5 correspond to predicted ordered regions/residues.

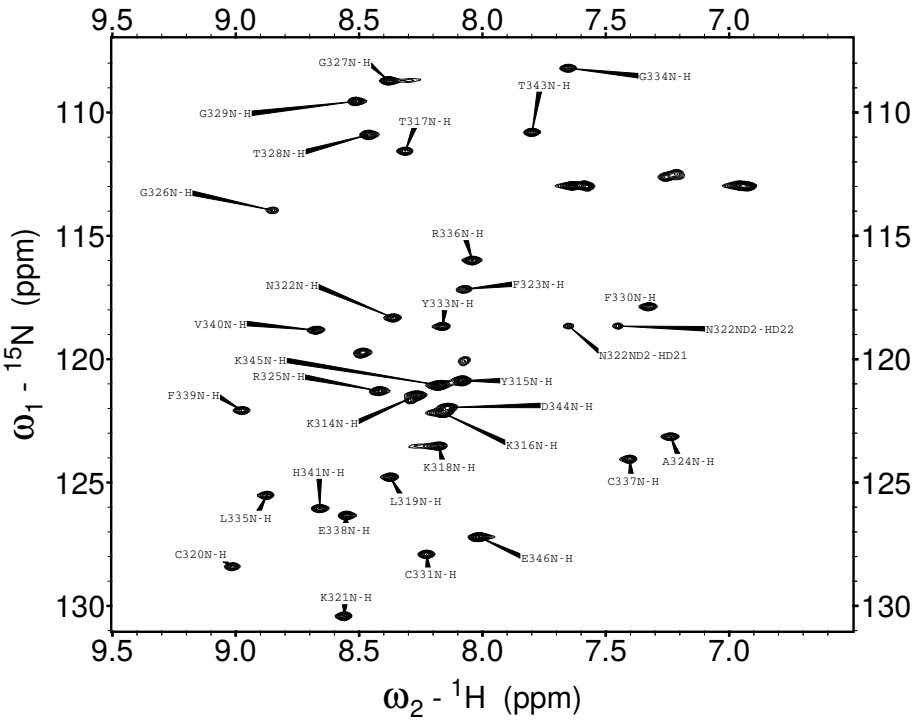

Figure S2: ^{15}N-^{1}H HSQC spectrum of MEX-5$_{312–346}$, containing only ZF2. For each H-N backbone resonance, the corresponding amino acid residue is indicated.

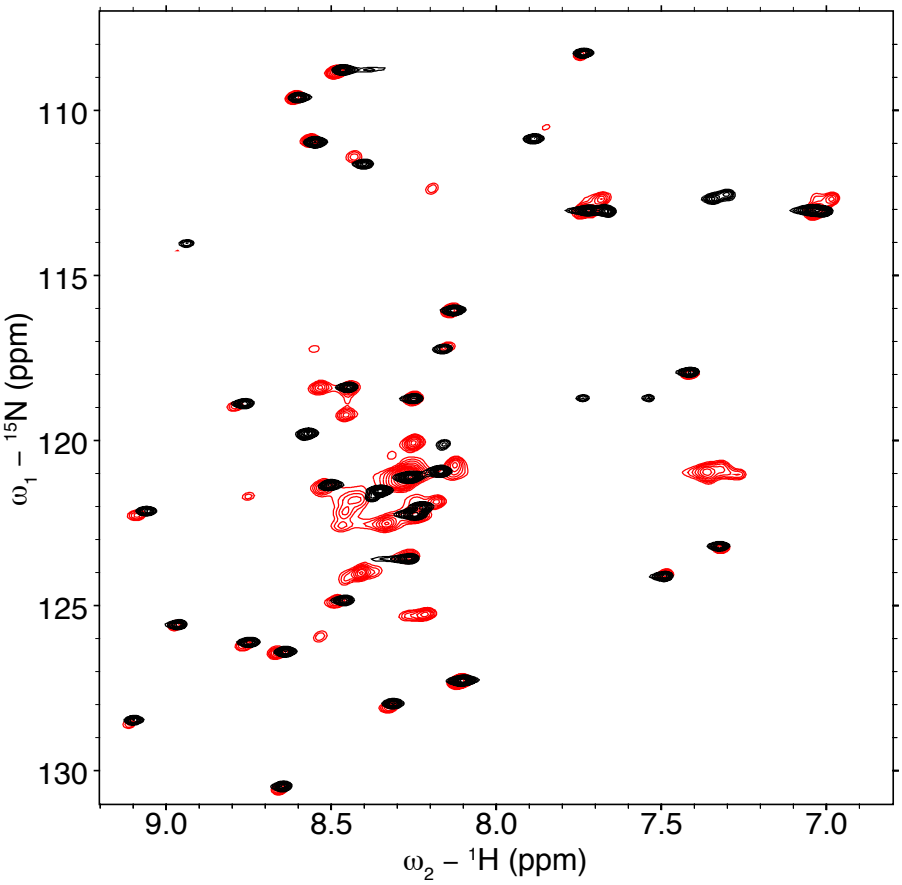

Figure S3: The ^{15}N-^{1}H HSQC spectrum of MEX-5$_{312-346}$ (black), containing only ZF2, has a similar number of cross-peaks and similar chemical shifts compared to the TZF domain (red).

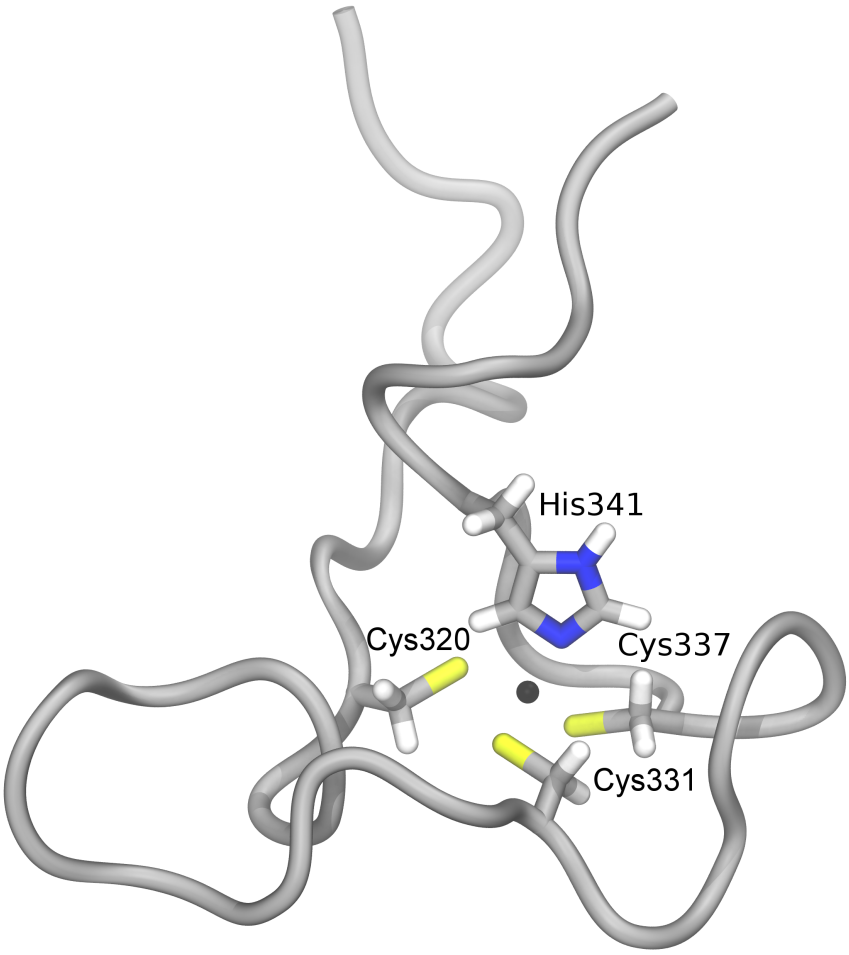

Figure S4: Solution structure of MEX-5 ZF2 showing the side chains of the zinc coordinating residues Cys 320, Cys 331, Cys 337 and His 341.

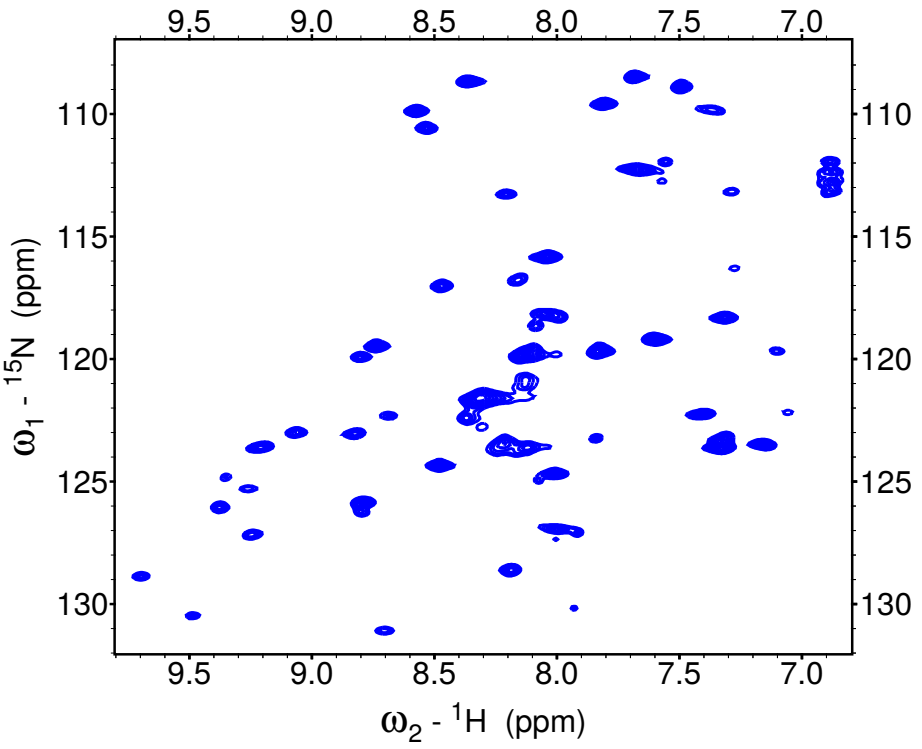

Figure S5: The ^{15}N-^{1}H HSQC spectrum of the TZF domain of MEX-5 bound to 5′-UUUUAUUUAUUUU-3′ RNA exhibits more cross-peaks than the RNA-free spectrum.

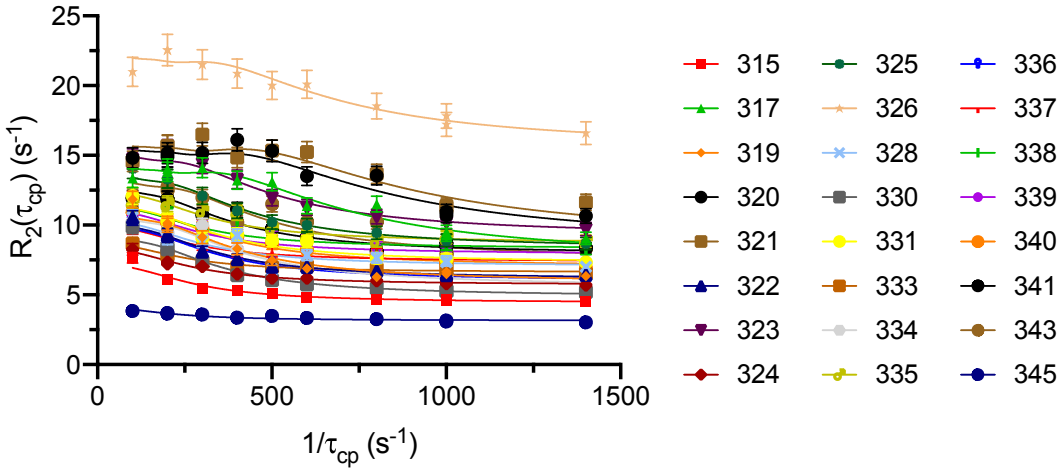

Figure S6: Chemical exchange for ZF2 of MEX-5. ^{15}N relaxation dispersion profiles measured for the residues of ZF2 of MEX-5 at 293 K and at a static magnetic field of 14.1 T. ^{15}N spin relaxation rate constants R_2 were calculated from the monoexponential decay fit of the cross-peak intenities; uncertainties were estimated by jackknife simulations. The solid lines represent the best global fit of the data obtained by optimizing k_{ex}, p_A, $\Delta\omega$ and R_2^0 to the following equation $R_2(\frac{1}{\tau_{\mathrm{cp}}}) = R_2^0 + \frac{1}{2}(k_{\mathrm{ex}} - \frac{1}{\tau_{\mathrm{cp}}}\cosh^{-1}(D_+\cosh(\eta_+) - D_-\cos(\eta_-))$, where $D_\pm = \frac{1}{2}(\pm 1 + \frac{\psi+2\Delta\omega^2}{(\psi^2+\zeta^2)^{1/2}})^{1/2}$, $\eta_\pm = \frac{\tau_{\mathrm{cp}}}{\sqrt{2}}(\pm\psi + (\psi^2+\zeta^2)^{1/2})^{1/2}$, $\psi = k_{\mathrm{ex}}^2 - \Delta\omega^2$, $\zeta = -2\Delta\omega k_{\mathrm{ex}}(p_A - p_B)$, $k_{\mathrm{ex}} = k_1 + k_{-1}$, with τ_{cp} being the delay between 180° pulses in the CPMG pulse train, p_{A} and p_{B} the populations of the two exchanging states A and B, $\Delta\omega$ their chemical shift difference and k_1 and k_{-1} the forward and reverse rate constants, respectively. The data was globally fitted as all residues shared the same k_{ex} and p_{A} values but different values of $\Delta\omega$ and R_2^0. From the global fit we obtained $k_{\mathrm{ex}} = 640 \pm 50$ s^{-1} and $p_{\mathrm{A}} = 0.989 \pm 0.001$.

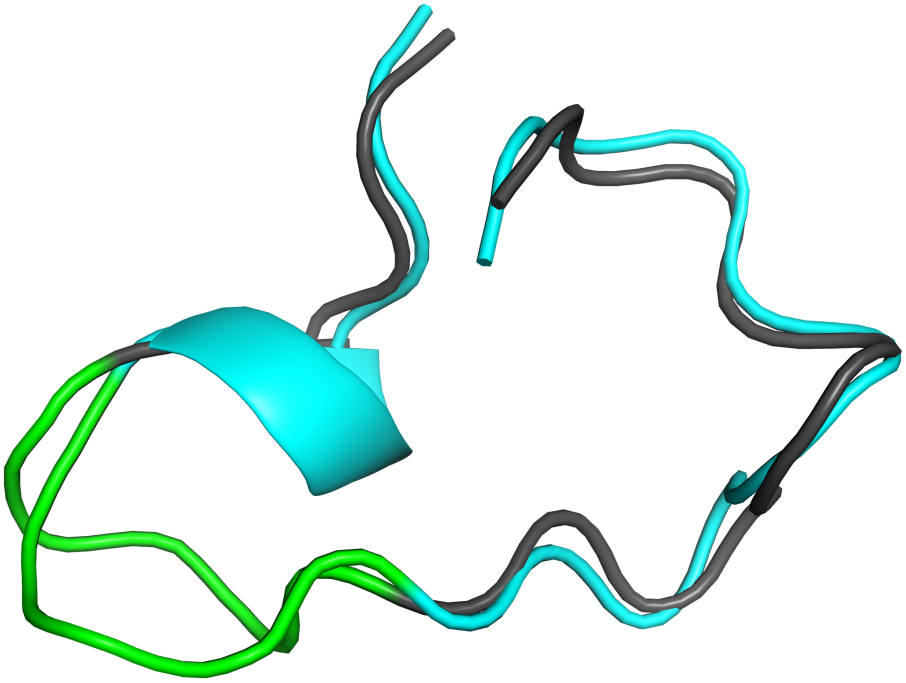

Figure S7: Overlay of the structure of ZF2 determined with NMR spectroscopy (cyan) and from a snapshots taken from the MD trajectory of MEX-5 (gray). The flexible glycine rich region (residues 325-329) is highlighted in green.

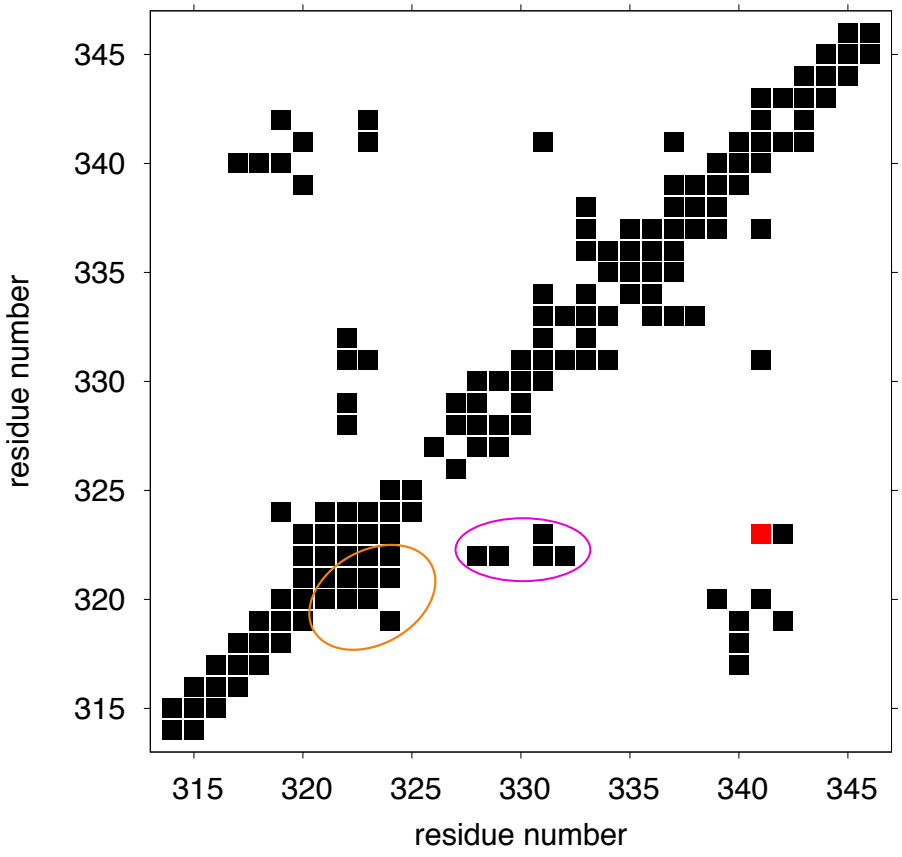

Figure S8: Plot illustrating the contact map calculated from the distance restraints, based on NOE resonances, generated by CYANA. The contact corresponding to the NOE between atoms Phe323-H$^{\delta}$ and His341-H$^{\delta 2}$ is indicated as a red square. Contacts corresponding to NOEs between the residues in the 321-324 region and between Asn322 and the residues in the 328-332 region are highlighted using orange and purple cirles, respectively.

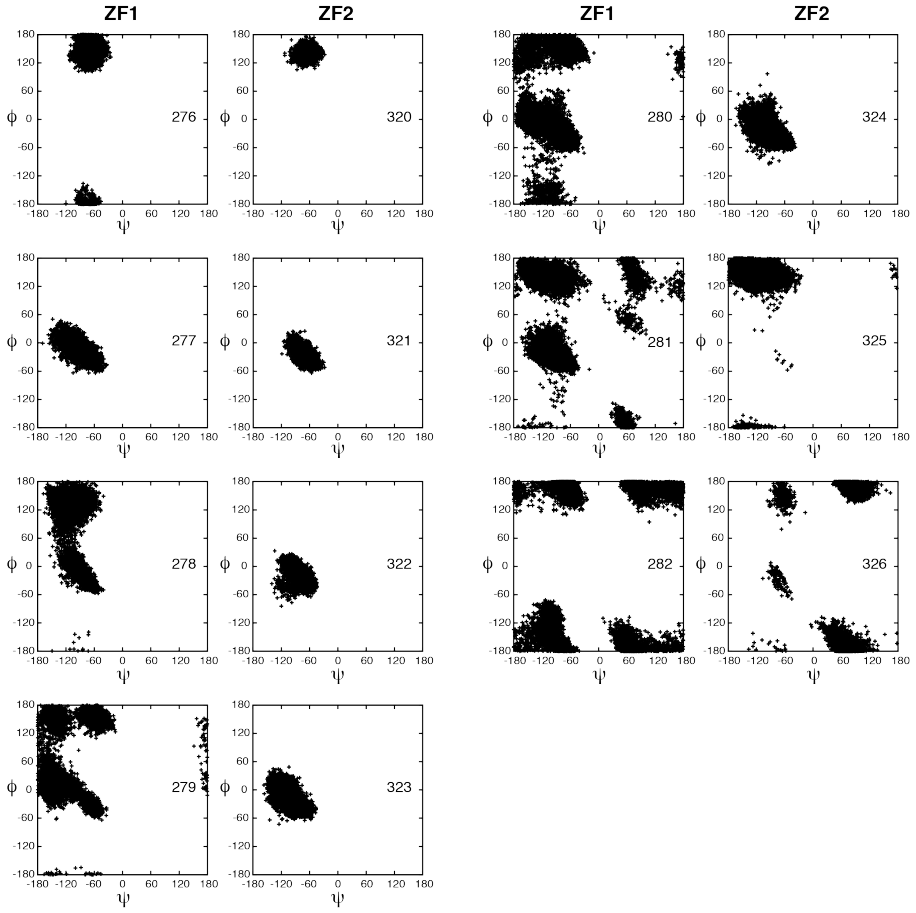

Figure S9: Backbone dihedral angles, ϕ and ψ. **A**. Backbone dihedral angles, ϕ and ψ, are plotted for corresponding residues located between the first and second cysteine residues in ZF1 and ZF2. The residue number is indicated on each plot.

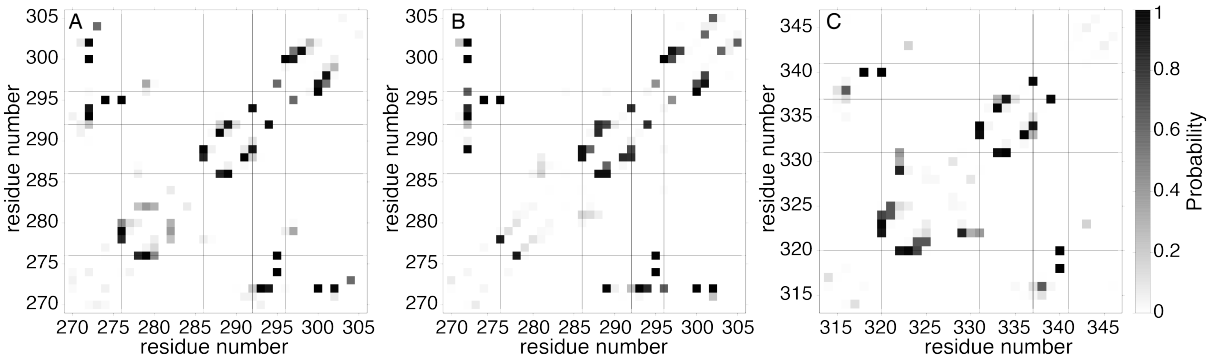

Figure S10: Hydrogen bond probabilities calculated for the residues of ZF1 and ZF2 of MEX-5. **A**. Hydrogen bond probabilities of ZF1 calculated using only the conformations of ZF1 where the side chain of H296 is stacked against the side chain of H279. **B**. Hydrogen bond probabilities of ZF1 calculated using the conformations of ZF1 where there is no stacking between the side chains of H296 and of H279. **C**. Hydrogen bond probabilities of ZF2.

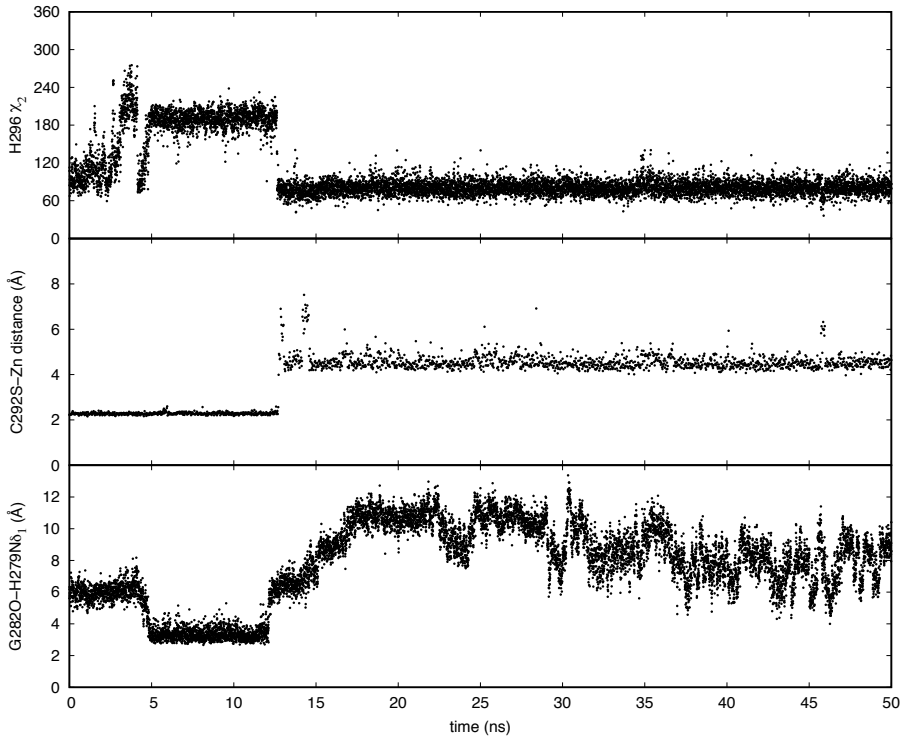

Figure S11: Plots illustrating the loss of Zn^{2+} coordination from ZF1 following the loss of the stacking interaction between H279 and H296. The χ_2 dihedral angle of the zinc-coordinating H296 (top panel), C292S $-$ Zn^{2+} distance (middle panel) and H279Nδ_1 $-$ G282O distance (bottom panel) are shown as functions of time. Stacking between the side chain of H279 and H296 occurs between 5 ns and 12 ns and maintains the H296 χ_2 dihedral angle to $\approx 180°$ (top). H279-H296 side chain stacking is facilitated by the formation of a hydrogen bond between the side chain of H279 and that of G282 (bottom). Loss of H279-H296 side chain stacking is followed by the loss of Zn^{2+} coordination (middle). Data are shown for one of the three MD trajectories of MEX-5.

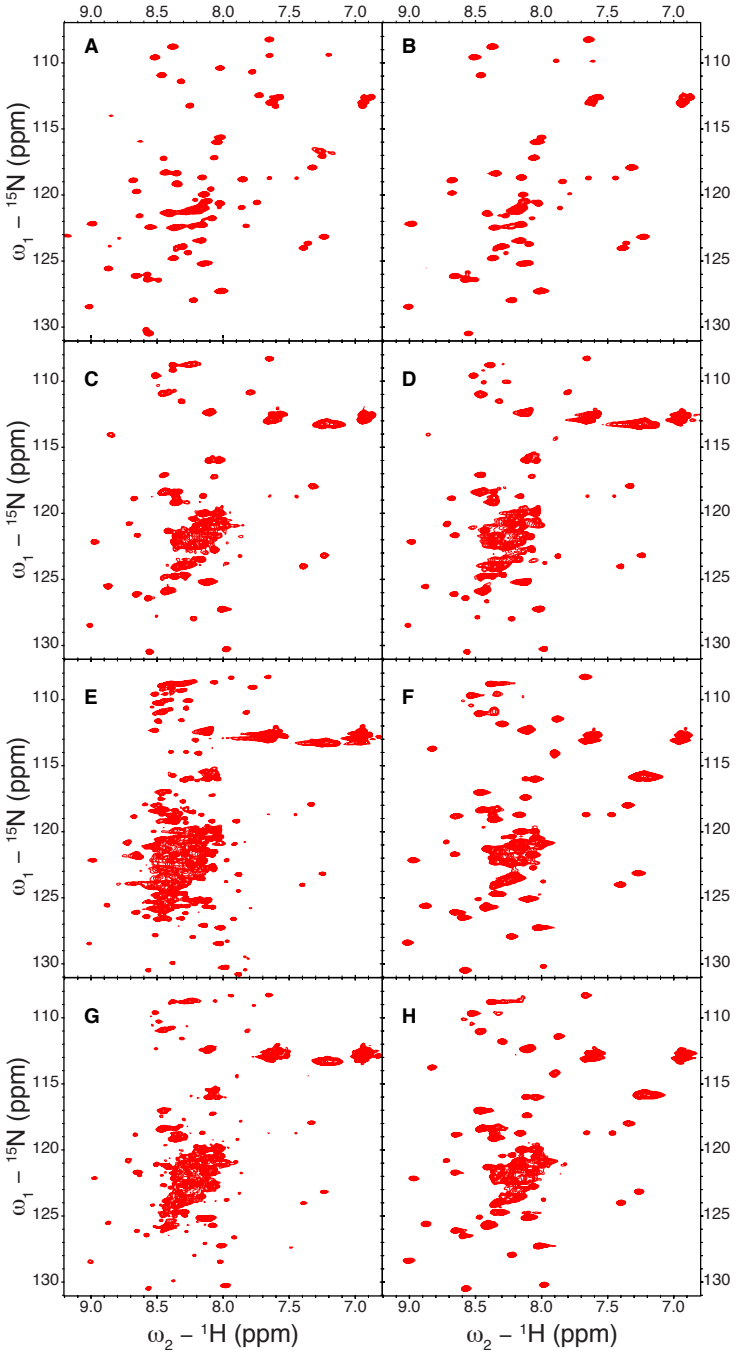

Figure S12: The TZF domain of MEX-5 mutants is not folded in the RNA-free state. The ^{15}N-^{1}H HSQC spectra of MEX-5 mutants from table 2: **A**:CMMFASGIKPC, **B**:CMMHASGIKAC, **C**: CMMHASGGIKPC, **D**: CMMHASGAIKPC, **E**: CMMHASGGIGPC, **F**: CMMHASGGTGPC, **G**: CMNHASGGIKPC, **H**: CMNHASGGIGPC. In panels E and G, the cluster of overlapped peaks in the middle of the spectra indicate aggregation.

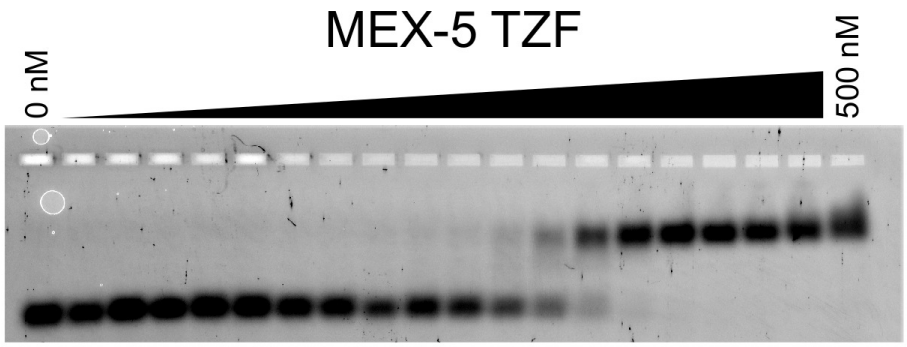

RNA sequence	MEX-5 TZF	$MEX\text{-}5_{CX10C}$ TZF
UUUUAUUUAUUUU	15±1 nM	9±1 nM
UUUUUUUUUUUUU	136±7 nM	154±4 nM
UUUUUUUUAUUUU	62±4 nM	77±6 nM
UUUUAUUUUUUUU	26±3 nM	48±5 nM

Figure S13: The TZF domains of MEX-5 and MEX-5_{CX10C} bind to the same targets with similar affinity. On top: the interaction of MEX-5 with ARE13 RNA as measured by EMSA. On bottom: The $K_{d,app}$ and the fit error of the two proteins are shown for the four RNA sequences.

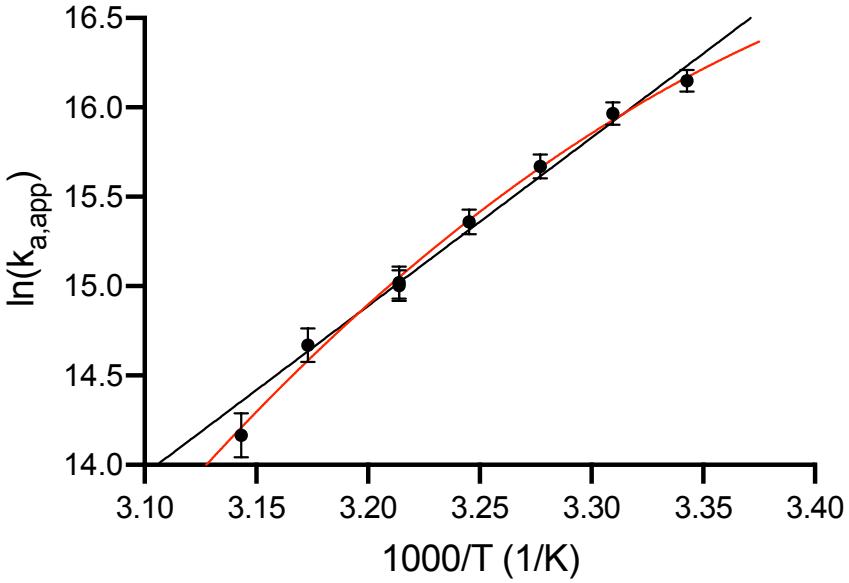

Figure S14: van't Hoff plot of ln $K_{a,app}$ as a function of 1/T measured for the TZF domain of MEX-5 with ARE13 RNA using fluorescence polarization. Bars represent the uncertainties propagated from the standard errors of the fits of $K_{d,app}$. The best fit of the data obtained from the linear fit (with $\Delta H = -18.7 \pm 0.9$ Kcal mol^{-1} and $\Delta S = -0.030 \pm 0.003$ Kcal mol^{-1} K^{-1}) and from a three parameter fit (with $\Delta H = -13 \pm 2$ Kcal mol^{-1}, $\Delta S = -0.010 \pm 0.006$ Kcal mol^{-1} K^{-1} and $\Delta C_p = -0.7 \pm 0.2$ Kcal mol^{-1} K^{-1} at a reference temperature of 298.15 K) are shown in black and red, respectively.